Infiltration in soils with a saturated surface

W. L. Hogarth,[1] D. A. Lockington,[2] D. A. Barry,[3] M. B. Parlange,[3] R. Haverkamp,[4] and J.-Y. Parlange[5]

[1] An earlier infiltration equation relied on curve fitting of infiltration data for the determination of one of the parameters, which limits its usefulness in practice. This handicap is removed here, and the parameter is now evaluated by linking it directly to soil-water properties. The new predictions of infiltration using this evaluation are quite accurate. Positions and shapes of soil-water profiles are also examined in detail and found to be predicted analytically with great precision.

1. Introduction and Theoretical Background

[2] The infiltration process of soil enters into most hydrological problems, e.g., irrigation, erosion, and weather forecasting, among many. Physically based infiltration equations go back at least to *Green and Ampt* [1911] equation, with greater understanding being obtained with *Richards* [1931] equation. Two very thorough reviews of most of the existing infiltration equations based on Richards equation can be found in *Basha* [2011] and in *Triadis and Broadbridge* [2010]. Those discussions will not be repeated here except when they impact this paper directly.

[3] The present paper continues an approach which is based on *Green and Ampt* [1911] and *Richards* [1931] equations. *Parlange et al.* [1982] introduced a three-parameter infiltration equation valid for a saturated soil surface. Those parameters are sorptivity, saturated conductivity, and an interpolation parameter δ, which goes from 0, when the equation reduces to zero obtained by *Green and Ampt* [1911], to 1 when the equation reduces to one obtained earlier by *Talsma and Parlange* [1972; see also *Smith and Parlange*, 1978]. This three-parameter equation is discussed in detail by *Basha* [2011] and *Triadis and Broadbridge* [2010] following new interpretations. A fourth parameter was introduced by *Haverkamp et al.* [1990] to represent ponding on the surface. *Barry et al.* [1995] used

this fourth parameter γ as a curve fitting parameter but simplified the equation by taking $\delta = 1$.

[4] As in *Barry et al.* [1995], we keep $\delta = 1$ even though values of δ less than one can be used to improve the agreement with numerical results for infiltration [*Parlange et al.*, 1985; *Basha*, 2011]. As this paper concentrates on a discussion of γ, we keep $\delta = 1$. In addition, for capillary rise $\delta = 1$ [*Kunze et al.*, 1985], and if δ is a true physical parameter, then the same value should hold for infiltration. However, it is quite easy to reintroduce δ in the equations if so desired.

[5] In a recent paper on time compression approximations (TCAs) by *Hogarth et al.* [2011], relationships between the cumulative infiltration I and the surface flux q were examined in detail based on an expansion procedure started by *Parlange et al.* [1997]. For the purpose of TCA, it was sufficient to consider the cases when either the surface flux or the surface water content is constant, even though the method can be applied for arbitrary surface conditions. In this paper, we are primarily concerned with infiltration and the profile determination following the same basic procedure [*Parlange et al.*, 1997]. The profiles are given by equation (1) [see, e.g., *Hogarth et al.* [2011, equation (2)].

$$\int_{\theta}^{\theta_s} \frac{D d\overline{\theta}}{q\overline{\theta}/\theta_s - k(\overline{\theta})} = z + Mz^2, \quad (1)$$

where θ is the water content at vertical position z, $z = 0$ at the surface with θ_s being the water content at $z = 0$ and time t. $D(\theta)$ and $k(\theta)$ are the soil-water diffusivity and conductivity, respectively. When $\theta_s = \theta_{\text{sat}}$ (the saturated value), M is taken as

$$2\int_0^{\theta_{\text{sat}}} \frac{D d\theta M}{q} = \frac{\int_0^{\theta_{\text{sat}}} (\theta_{\text{sat}} - \theta) D d\theta}{\int_0^{\theta_{\text{sat}}} \theta D d\theta}. \quad (2)$$

[6] For constant q, the M-term is negligible [*Hogarth et al.*, 2011; see also *Sivapalan and Milly*, 1989]. For simplicity, we assume that the initial water content θ_i can be taken

---

[1]Faculty of Science and IT, The University of Newcastle, Callaghan, New South Wales, Australia.

[2]National Centre for Groundwater Research and Training, School of Civil Engineering, The University of Queensland, St Lucia, Queensland, Australia.

[3]Ecole polytechnique fédérale de Lausanne (EPFL), Faculté de l'environnement naturel, architectural et construit, Institut d'ingénierie de l'environnement, Lausanne, Switzerland.

[4]University Grenoble 1, CNRS, URA 1512, IMG, LTHE, Grenoble, France.

[5]Department of Biological and Environmental Engineering, Cornell University, Ithaca, New York, USA.

Corresponding author: J.-Y. Parlange, Department of Biological and Environmental Engineering, Cornell University, Ithaca, NY 14853, USA. (jp58@cornell.edu)
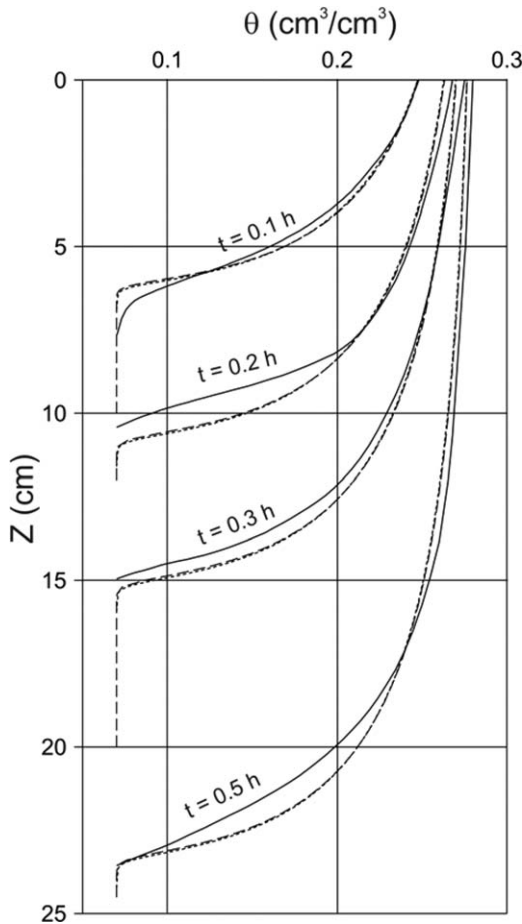
Figure 1. Water profiles in a Grenoble sand for constant flux at the surface. The solid lines represent experimental observations [*Boulier et al.*, 1984]. The numerical predictions, dotted lines, and the analytical results from equations (1) and (3) with $M = 0$, dashed lines, are essentially identical.

as constant. As a result, θ stands for the water content minus θ_i. Similarly, k and q stand for the conductivity and flux minus the conductivity at θ_i. Taking a nonuniform initial water content introduces complications in writing the equations but with no theoretical difficulties, following the approach of *Boulier et al.* [1984].

[7] It is important to note that neglecting M for constant q is necessarily approximate as $M = 0$ is exact only when q/θ_s is independent of time [*Fleming et al.*, 1984]. There have been many papers exploring the accuracy of equation (1) with $M = 0$ for constant q and possible alternatives to the use of $q\bar{\theta}/\theta_s$ in the integral [see, e.g., *Kutilek*, 1980; *Boulier et al.*, 1984; *Si and Kachanoski*, 2000; *Evanselides et al.*, 2005]. The conclusion is that in practice, the use of $q\bar{\theta}/\theta_s$ is very accurate, in agreement with the suggestion originally made in equation (8) of *Parlange* [1972], as long as the initial water content is not too large [*Boulier et al.*, 1984].

[8] Figure 1 summarizes the case considered by *Boulier et al.* [1984] and *Parlange et al.* [1985] for constant q using a Grenoble sand whose properties are given in those two papers. The numerical and analytical results are essentially undistinguishable in Figure 1. This was not the case with *Boulier et al.* [1984] and *Parlange et al.* [1985], where nu-

merical results showed dispersion near the wetting front. Here the numerical results were obtained using COMSOL finite element numerical software (COMSOL Multiphysics, version 3.5a, 2008, COMSOL. Inc., http://www.comsol.com/). This software eliminated the numerical dispersion and thus can be trusted to provide accurate solutions at the wetting front. Note that using equation (1) with $M = 0$ requires the knowledge of $\theta_s(t)$ which is obtained by conservation of mass, integrating equation (1) to obtain

$$\int_0^{\theta_s} \frac{D\theta d\theta}{q\theta/\theta_s - k} = qt. \tag{3}$$

[9] Note also that the measured profiles differ slightly from the predicted profiles simply reflecting that the properties, obtained from many experiments, were not exactly those of the particular soil sample used for the experiment in Figure 1. Experimental scatter of this nature is not unexpected and is sometimes used, wrongly, to justify poor approximate analytical solutions. Rather, analytical approximations should be as accurate as possible so that differences with observations are unambiguously linked to experimental uncertainties and not to inaccurate models. The solution for constant q and $M = 0$ will be used later for comparison to the solution with $M \neq 0$.

2. Cumulative Infiltration and Flux With Surface Saturation

[10] We are now using the profiles with $M \neq 0$, given by equation (2) and $\theta_s = \theta_{sat}$. The first step is to derive the equivalent to equation (3) to obtain $q(t)$. Several expressions have been used in the past that related I and q. Equation (20) of *Hogarth et al.* [2011] gave

$$\int_0^{\theta_{sat}} \frac{D\theta d\theta}{q\theta/\theta_{sat} - k} = I + \int_0^{\theta_{sat}} (\theta_{sat} - \theta)Dd\theta/2q. \tag{4}$$

[11] The last term is an approximation of $M \int_0^{\theta_{sat}} z^2 d\theta$ for short times, such that $Iq \simeq S^2/2$, where S is the sorptivity approximated by

$$S^2 \simeq \int_0^{\theta_{sat}} D(\theta_{sat} + \theta)d\theta. \tag{5}$$

[12] Equation (4) is identical, with minor notation differences, with equation (9) of *Parlange et al.* [1982]. If one ignored the M-term altogether, then the first term in equation (4) would have to be corrected for the resulting equation to hold in the short time to obtain equation (18) of *Barry et al.* [2007]:

$$\left(\frac{S^2}{2\theta_{sat}} \int_0^{\theta_{sat}} Dd\theta\right) \int_0^{\theta_{sat}} \frac{D\theta d\theta}{q\theta/\theta_{sat} - k} = I. \tag{6}$$

[13] Finally, equation (6) can be modified to take into account a small negative potential h_{str}, with the soil

remaining saturated for $h > -|h_{str}|$. Conceptually, $|h_{str}|$ can be associated with the largest pores in the soil [*Haverkamp et al.*, 1990]. In practice, the value of $|h_{str}|$ cannot be measured independently and instead was obtained by curve fitting infiltration data [*Barry et al.*, 1995]. Equation (6) then becomes

$$\frac{S^2}{2\theta_{sat}\int_0^{\theta_{sat}} Dd\theta}(1-\gamma)\int_0^{\theta_{sat}}\frac{D\theta d\theta}{q\theta/\theta_{sat}-k}=I-\frac{\gamma S^2/2}{q-k_{sat}}, \quad (7)$$

where

$$\gamma = \frac{-2k_{sat}h_{str}\theta_{sat}}{S^2}. \quad (8)$$

[14] Note that in equation (7) of *Barry et al.* [1995] and equation (16) of *Haverkamp et al.* [1990], the equations were further simplified by assuming

$$\frac{D}{\theta_{sat}}\int_0^{\theta_{sat}} Dd\theta = \frac{d(k/\theta)/d\theta}{k_{sat}}. \quad (9)$$

[15] Since k increases rapidly with θ, k/θ is hardly different from k/θ_s. Making that substitution in equation (9) and combining it with $D = kdh/d\theta$, where h is the potential, leads to an exponential dependence of k on h, i.e., the standard Gardner relation. Thus, in our case, equation (9) implies a soil hardly different from a Gardner soil. It is clear that eliminating D from the integral of equation (7), using equation (9), results in an integral, where k/θ is the variable, which can be integrated explicitly as done by *Barry et al.* [1995] and *Haverkamp et al.* [1990]. This simplification will be discussed further later on.

[16] In the present paper, the soil surface is taken at a zero potential. There is no difficulty to include a ponding term $h_{surf} > 0$ which is simply added to $|h_{str}|$ as done by *Haverkamp et al.* [1990] and *Barry et al.* [1995]. It is not considered here as it corresponds only to changing the value of γ.

[17] Altogether, we consider two possible relations between I and q, equations (4) and (7), which could be simplified using equation (9). Equation (6) is, of course, just equation (7) with $\gamma = 0$. Obviously, for the Grenoble sand used for our illustration, $|h_{str}|$ and γ are physically equal to zero. However, *Barry et al.* [1995] took a nonzero, and hence nonphysical value to improve infiltration prediction, keeping γ only as a curve-fitting parameter. In the following, we first discuss the results obtained from equation (4). Then, we follow the same approach starting with equation (7) and compare the results.

[18] Since we paid special attention to short-time infiltration to obtain equation (4), we are first considering the Taylor expansion of the equation for large q, keeping the first two terms only. Equation (4) yields

$$Iq \simeq S^2/2 + \theta_{sat}^2 \int_0^{\theta_{sat}} k(D/\theta)d\theta/q. \quad (10)$$

[19] Finally, we can simplify equation (4) using equation (9) to obtain

$$I = \frac{\theta_{sat}\int_0^{\theta_{sat}} Dd\theta}{k_{sat}}\ln\frac{q}{q-k_{sat}} - \int_0^{\theta_{sat}}(\theta_{sat}-\theta)\frac{Dd\theta}{2q}. \quad (11)$$

[20] To obtain the relationships between q and t, we differentiate equation (4) with respect to time, replacing dI/dt by q, to obtain a differential equation for q which is easily integrated to obtain

$$t = \int_0^{\theta_{sat}}\frac{D\theta^2}{k^2\theta_{sat}}\ln\left(\frac{q\theta/\theta_{sat}-k}{q\theta/\theta_{sat}}\right)d\theta + \int_0^{\theta_{sat}}\frac{D\theta^2 d\theta}{k\theta_{sat}(q\theta/\theta_{sat}-k)}$$
$$- \frac{1}{4q^2}\int_0^{\theta_{sat}}(\theta_{sat}-\theta)Dd\theta, \quad (12)$$

and using equation (9) in the two integrals so that only k/θ enters as variable, we obtain

$$t = \frac{\theta_{sat}\int_0^{\theta_{sat}} Dd\theta}{k_{sat}^2}\left(\ln\frac{q}{q-k_{sat}}-\frac{k_{sat}}{q}\right)-\frac{1}{4q^2}\int_0^{\theta_{sat}}(\theta_{sat}-\theta)Dd\theta. \quad (13)$$

[21] Starting now with equation (7), we proceed as before; the Taylor expansion for large q, keeping the first two terms only, or

$$Iq \simeq S^2/2 + \left[\left(S^2/2\theta_{sat}\int_0^{\theta_{sat}} Dd\theta\right)\theta_{sat}^2\int_0^{\theta_{sat}} k(D/\theta)d\theta(1-\gamma)\right.$$
$$\left. + \gamma S^2 k_{sat}/2\right]/q. \quad (14)$$

[22] Note that for $\gamma = 0$, equations (10) and (14) differ by the term

$$1 - \left(\frac{S^2}{2\theta_{sat}}\int_0^{\theta_{sat}} Dd\theta\right) \simeq \frac{\int_0^{\theta_{sat}}(\theta_{sat}-\theta)Dd\theta}{2\int_0^{\theta_{sat}}\theta_{sat} Dd\theta}, \quad (15)$$

which is small. In all our estimates, we keep terms up to that small order and ignore terms of higher order, i.e., square terms.

[23] If we use equation (9) to estimate the I/q terms in equation (14), then equation (14) reduces to equation (10) if we take

$$\gamma = \gamma_0 = \int_0^{\theta_{sat}}(\theta_{sat}-\theta)Dd\theta/2\theta_{sat}\int_0^{\theta_{sat}} Dd\theta. \quad (16)$$

[24] Finally, we simplify equation (7) when equation (9) holds and obtain
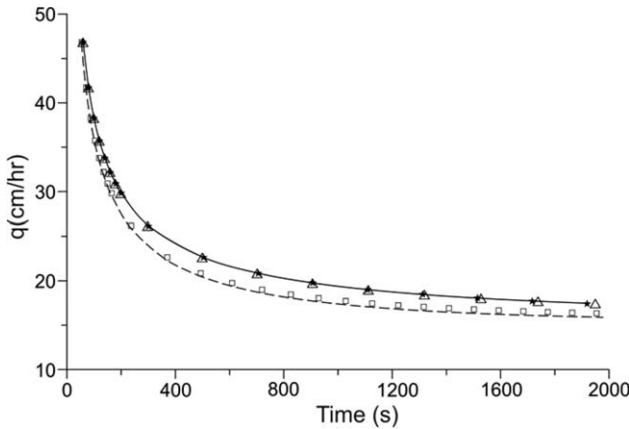
Figure 2. Fluxes for a saturated soil surface. Numerical results (solid line) and analytical approximations: stars with equation (12), squares with equation (13), triangles with equation (18), and dashed line with equation (19). In both equations (18) and (19), $\gamma = \gamma_0 = 0.05$ from equation (16).

$$I = \frac{S^2}{2k_{sat}}(1-\gamma)1n\frac{q}{q-k_{sat}} + \frac{\gamma S^2}{2(q-k_{sat})}. \qquad (17)$$

[25] We now differentiate equation (7) with respect to time and integrate the resulting differential equation to obtain

$$t = \frac{S^2(1-\gamma)}{2\theta_{sat}\int_0^{\theta_{sat}} Dd\theta}\left[\int_0^{\theta_{sat}}\frac{D\theta^2}{k^2\theta_{sat}}1n\left(\frac{q\theta/\theta_{sat}-k}{q\theta/\theta_{sat}}\right)d\theta \right.$$
$$\left. + \int_0^{\theta_{sat}}\frac{D\theta^2 d\theta}{k\theta_{sat}(q\theta/\theta_{sat}-k)}\right] - \frac{\gamma S^2}{2k_{sat}^2}\left(1n\frac{q}{q-k_{sat}}-\frac{k_{sat}}{q-k_{sat}}\right),$$

$$(18)$$

and with equation (9)

$$t = \frac{S^2}{2k_{sat}^2}\left[(1-2\gamma)1n\frac{q}{q-k_{sat}}-(1-\gamma)\frac{k_{sat}}{q}\right] + \frac{\gamma S^2}{2k_{sat}(q-k_{sat})}. \qquad (19)$$

[26] Figure 2 compares $q(t)$ given by equations (12), (13), (18), and (19) with γ from equation (16) equal to 0.05, with the numerical results.

[27] Several results are apparent. First, equation (12) provides an excellent approximation for $q(t)$ when compared to the numerical results. The results predicted by equation (18) are equally good if we take $\gamma = \gamma_0 = 0.05$ as given by equation (16). Interestingly, equations (13) and (19) are still in basic agreement with each other, with $\gamma = 0.05$, but they differ significantly from the numerical results. This discrepancy simply shows that the Gardner-type relation of equation (9) is not exact for the Grenoble sand, and not surprisingly, this assumption affects equations (18) and (19) in a similar manner.

[28] We know [*Barry et al.*, 1995] that equation (19) can be curve fitted accurately but only by using a γ differently from γ_0. Of course, equation (19) is easy to use in practice once γ is known as it relies only on the knowledge of

two additional parameters S and k_{sat} (besides γ), whereas equation (12) requires the estimations of two integrals (based on knowing D and k of θ) for each value of the flux q. Furthermore, equation (19) can be used easily in the case of infiltration with ponding [*Barry et al.*, 1995].

[29] The main inconvenience of using equation (19) as in *Barry et al.* [1995] is that γ in that paper had to be obtained by curve fitting as the theoretical value of equation (16) shows poor accuracy (see Figure 2). Instead, we are now going to estimate a constant value of γ, i.e., independent of the flux, based on soil properties. For that purpose, we first remember that as shown in Figure 2, equation (7) is in good agreement with both the numeric and equation (4) for $\gamma = \gamma_0 = 0.05$. Then, the result for large q, i.e., equation (11) with $\gamma = \gamma_0 (= 0.05)$, is taken as equal to the result for $\gamma \neq \gamma_0$ but obtained when equation (9) is used. This straightforward calculation gives

$$\gamma = \frac{2\theta_{sat}}{k_{sat}\int_0^{\theta_{sat}} Dd\theta}\int_0^{\theta_{sat}}\frac{kD}{\theta}d\theta(1-\gamma_0) + 2\gamma_0 - 1. \qquad (20)$$

[30] Of course, if equation (9) truly holds, equation (20) yields $\gamma = \gamma_0$. For our particular example, this gives instead $\gamma = 0.39$, and as shown in Figure 3, this value, when used in equation (19), gives a very good estimate of $q(t)$ as expected.

[31] To estimate the sensitivity of the results to the value of γ, a slightly different value, $\gamma = 0.33$, is also considered. This value was chosen by curve fitting equation (19) to the numerical results for $t \rhd 1000$s, when $\gamma = 0.39$ is not quite as good. However, $\gamma = 0.39$ is clearly better on average, if we combine equations (17) and (19) to predict $I(t)$, then as shown in Figure 4, the choice of $\gamma = 0.39$ is neatly superior to that of $\gamma = 0.33$. Altogether, then, equation (20) gives an adequate physical estimate of γ, requiring no curve fitting to predict either $I(t)$ or $q(t)$ with the very simple equations given in equations (17) and (19).
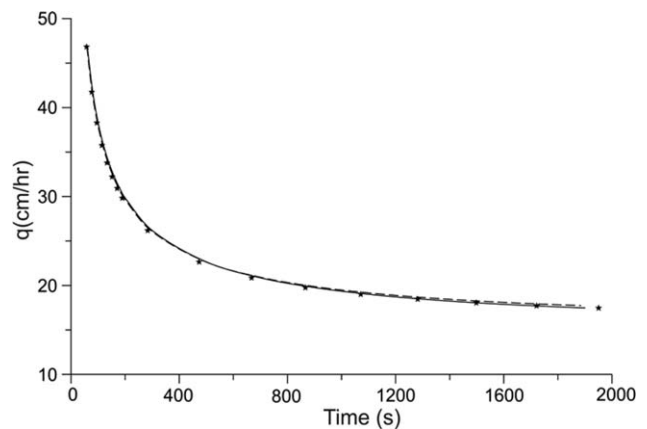
Figure 3. Fluxes obtained numerically (solid line) and from equation (19): dashed line with $\gamma = 0.39$ from equation (20) and stars with $\gamma = 0.33$ obtained by curve fitting for long times.
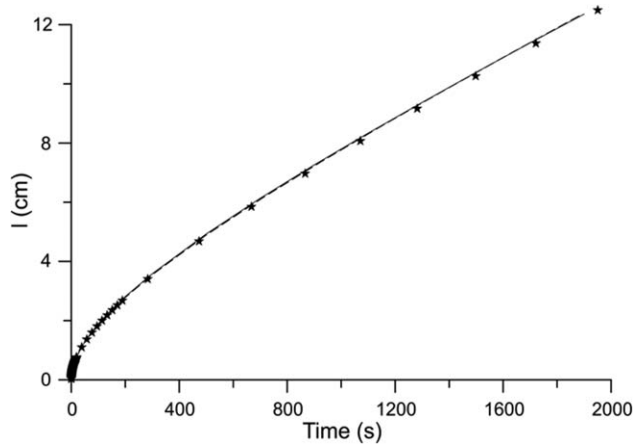
Figure 4. Infiltration I as a function of time obtained numerically (solid line) or analytically, combining equations (17) and (19) for $\gamma = 0.33$ (stars) and $\gamma = 0.39$ (dashed line).

3. Water Content Profiles

[32] We are primarily interested in assessing the impact of the z^2-term on the profile given by equation (1). The use of equation (1) means that at the difference of our results for I or q, we do not attempt to obtain $\theta(z)$ in terms of a few simple physical parameters. Instead, we require to integrate the left-hand side of equation (1) for each value of q, i.e., time. Our estimates of I and q were based on equation (1); hence, it is important to check the accuracy of equation (1) in predicting $\theta(z, t)$. In this paper, we carried out the calculation of the I and q estimates first, since applying equation (1) requires knowing $q(t)$. This section is more of theoretical interest like equation (1), whereas I and q as given by equations (17) and (19), using equations (16) and (20) for γ_0 and γ, are simple and of greater practical interest.

[33] For the illustration, we consider a flux $q = 50$ cm/h with either equation (12) or (19) giving $t = 51.1$ s. Note that our illustration is for a short time, i.e., a large q. As shown in equation (2), this enhances the M-value and hence the impact of the z^2-term on the profile, which we try to assess. This means that without the z^2-term, we can also compare with the profile obtained at ponding with a constant flux of $q = 50$ cm/h, since the chosen flux is larger than k_{sat}.

[34] Using equation (3) with $\theta_s = \theta_{\text{sat}}$ gives the time at ponding, $t_p = 97.56$ s, i.e., about twice the time, 51.1 s, when $q = 50$ cm/h for $\theta_s = \theta_{sat}$ for all times. This, of course, is because when $\theta_s = \theta_{\text{sat}}$, q is larger than $q = 50$ cm/h for $t < 51.1$ s, and for infiltration with $q = 50$ cm/h, a longer time is required to accumulate a similar amount of water. At 97.6 s, the amount of water is $I = qt_p = 1.355$ cm, whereas equation (4), for $\theta_s = \theta_{\text{sat}}$, gives $I = 1.297$ cm, which is 4.5% less than 1.355 cm due to the last small term in equation (4). The results are shown in Figure 5a and with more details near the wetting front in Figure 5b. On Figure 5b, the slight differences between the analytical results and the numerics are visible (they are not in Figure 5a).

[35] If we now look at the profile, with the z^2-term, but for $I = 1.355$ cm, then the time is obviously longer, 55.3 s,

and the flux smaller, 48.52 cm/h. The two profiles for $I = 1.355$ cm, one with z^2 for $\theta_s = \theta_{\text{sat}}$, and one without z^2 for constant flux, $q = 50$ cm/h, are very close in shape. Hence, the presence of the z^2-term affects the position of the profiles significantly, by 4.5%, but not their shape. We note that the z^2-term reduces the estimate of z, and the more so as z is larger making the profile more "square" as shown in Figures 5a and 5b.

[36] As also shown in Figures 5a and 5b, there is an excellent agreement between analytical and numerical results. The analytical results are somewhat complex, and to get some physical insight in the infiltration process, we are going to use some simplifications which make the results more transparent and are still quantitatively
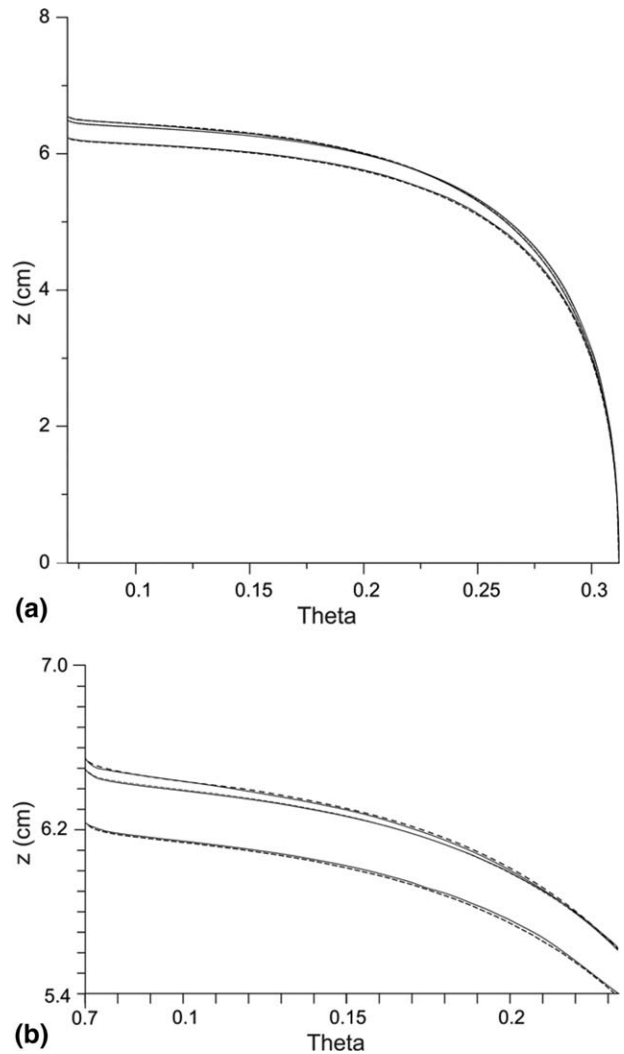
Figure 5. Comparison of profiles $z(\theta)$ for saturated surface and constant flux. (a) Profiles over the whole range of θ, showing little difference between the numerics (solid lines) and analysis (dashed lines). (b) Details of the profiles near the fronts. In descending order, from the top: (1) profiles for constant q, i.e., without the z^2-term, when $q = 50$ cm/h and $I = 1.355$ cm at ponding; (2) profiles when $\theta_s = \theta_{\text{sat}}$ at all times when $I = 1.355$ cm, with the z^2-term; and (3) profiles when $\theta_s = \theta_{\text{sat}}$ at all times when $q = 50$ cm/h, with the z^2-term.

appropriate. The constant flux profile is given subscript 1, the profiles for $\theta_s = \theta_{sat}$ are assigned 2 and $*$ for $q = 50$ cm/h and for $I = 1.355$ cm, respectively. To be specific, we consider the front positions, denoted with subscript f, and we see in Figure 5 that z_{1f}, z_{2f}, and z_{*f} are close, and $(z_{1f} - z_{2f})$ is an order of magnitude smaller and $(z_{1f} - z_{*f})$ is another order of magnitude smaller.

[37] To the lowest order, as long as $q\theta/\theta_s$ is not too close to k, equation (1) shows that the front locations are in the vicinity of

$$z_f \simeq \frac{\int_0^{\theta_{sat}} D d\theta}{q - k_s}, \tag{21}$$

which for the present example, equals 6.2 cm, which is roughly correct. Then,

$$z_{1f} - z_{2f} \simeq M z_f^2 \tag{22}$$

[38] or from equations (2) and (21),

$$z_{1f} - z_{2f} \simeq \frac{q/2}{(q - k_s)^2} \int_0^{\theta_{sat}} \left(\frac{1 - \theta}{\theta_{sat}}\right) D d\theta \tag{23}$$

which is basically smaller than z_f by an order of $\gamma_0 q/(q - k_s) \simeq 0.073$ so that $z_{1f} - z_{2f} \simeq 0.45$ cm, which is roughly correct (slightly too large).

[39] The value of $(z_{1f} - z_{*f})$, as shown in Figure 5b, is very small. Using order of magnitude estimates (calculations available upon request), we obtain

$$(z_{1f} - z_{*f}) \simeq (z_{1f} - z_{2f})2\gamma. \tag{24}$$

[40] This shows that $(z_{1f} - z_{*f})$ is an order of magnitude less than $(z_{1f} - z_{2f})$ as obtained numerically. For the case of Figure 5b, equation (24) yields $(z_{1f} - z_{*f}) \simeq 0.045$ cm, which is basically correct and only very slightly too small.

4. Conclusion

[41] In practice, i.e., in the field, one is primarily interested in knowing I and q as a function of time, which is why this paper is primarily devoted to finding an appropriate γ to be used in equations (17) and (19). Originally [*Barry et al.*, 1995], this third parameter was obtained by curve fitting to infiltration data. Here we derived instead a theoretical relation in equation (20) giving γ in terms of soil properties so that no empirical curve fitting is necessary. Analytical and numerical results were found to be in excellent agreement using a Grenoble sand for illustration.

[42] The method is based on equation (1) giving the water content θ as a two-term expansion in z and z^2. For the Grenoble sand illustration, we checked that the profiles, numerical and analytical, are in excellent agreement using $q(t)$ as determined in equation (19). We found that the z^2-

term affects primarily the position of the profile rather than its shape. Finally, we derived some very simple expressions showing the relative positions of the wetting fronts, which provide a good physical insight in the infiltration process, either under constant flux or constant water content at the surface. An interesting result is that the shapes remain very similar for both cases, but positions have to be assessed carefully.

References

Barry, D. A., J.-Y. Parlange, R. Haverkamp, and P. J. Ross (1995), Infiltration under ponded conditions: 4. An explicit predictive infiltration formula, *Soil Sci.*, *160*, 8–17.

Barry, D. A., et al. (2007), Infiltration and ponding, in *Encyclopedia of Life Support Systems*, edited by J. A. Filar, pp. 322–346, Eolss Publ., Oxford.

Basha, H. A. (2011), Infiltration models for semi-infinite soil profiles, *Water Resour. Res.*, *47*, W08516, doi:10.1029/2010WR010253.

Boulier, J. F., J. Touma, and M. Vauclin (1984), Flux-concentration relation-based solution of constant-flux infiltration equation: 1. Infiltration into nonuniform initial moisture profiles, *Soil Sci. Soc. Am. J.*, *48*(2), 245–251.

Evanselides, C., C. Tzimopoulos, and G. Arampatzi (2005), Flux-saturation relationship for unsaturated horizontal flow, *Soil Sci.*, *170*(9), 671–679.

Fleming, J. F., J.-Y. Parlange, and W. L. Hogarth (1984), Scaling of flux and water content relations: Comparison of optimal and exact results, *Soil Sci.*, *137*(6), 464–468.

Green, W. H., and G. A. Ampt (1911), Studies on soil physics. Part I: The flow of air and water through soils, *J. Agric. Sci.*, *4*, 1–24.

Haverkamp, R., J.-Y. Parlange, J. L. Starr, G. Schmitz, and C. Fuentes (1990), Infiltration under ponded conditions: 3. A predictive equation based on physical parameters, *Soil Sci.*, *149*, 292–300.

Hogarth, W. L., D. A. Lockington, D. A. Barry, M. B. Parlange, G. C. Sander, L. Li, R. Haverkamp, W. Brutsaert, and J. Y. Parlange (2011), Analysis of time compression approximations, *Water Resour. Res.*, *47*, W09501, doi:10.1029/2010WR010298.

Kunze, R. J., J.-Y. Parlange, and C. Rose (1985), A comparison of numerical and analytical techniques for describing capillary rise, *Soil Sci.*, *139*(6), 491–496.

Kutilek, M. (1980), Constant-rainfall infiltration, *J. Hydrol.*, *45*(3–4), 289–303.

Parlange, J.-Y. (1972), Theory of water movement in soils: 8. One-dimensional infiltration with constant flux at the surface, *Soil Sci.*, *114*(1), 1–4.

Parlange, J.-Y., I. G. Lisle, R. D. Braddock, and R. E. Smith (1982), The three parameter infiltration equation, *Soil Sci.*, *133*, 337–341.

Parlange, J.-Y., W. L. Hogarth, J. F. Boulier, J. Touma, R. Haverkamp, and G. Vachaud (1985), Flux and water content relation at the soil surface, *Soil Sci. Soc. Am. J.*, *49*(2), 285–288.

Parlange, J.-Y., D. A. Barry, M. B. Parlange, W. L. Hogarth, R. Haverkamp, P. J. Ross, L. Ling, and T. S. Steenhuis (1997), New approximate analytical technique to solve Richards' equation for arbitrary surface boundary conditions, *Water Resour. Res.*, *33*(4), 903–906.

Richards, L. A. (1931), Capillary conduction of liquids through porous mediums, *Phys. A—J. Gen. Appl. Phys.*, *1*, 318–333.

Si, B. C., and R. G. Kachanoski (2000), A new solution for water storage to a fixed depth for constant flux infiltration, *Soil Sci. Soc. Am. J.*, *64*(1), 24–29.

Sivapalan, M., and P. C. D. Milly (1989), On the relationship between the time condensation approximation and the flux concentration relation, *J. Hydrol.*, *105*(3–4), 357–367.

Smith, R. E., and J.-Y. Parlange (1978), Parameter-efficient hydrologic infiltration-model, *Water Resour. Res.*, *14*, 533–538.

Talsma, T., and J.-Y. Parlange (1972), One-dimensional vertical infiltration, *Aust. J. Soil Res.*, *10*, 143–150.

Triadis, D., and P. Broadbridge (2010), Analytical model of infiltration under constant-concentration boundary conditions, *Water Resour. Res.*, *46*, W03526, doi:10.1029/2009WR008181.